

CHAPTER 8

**Structure based virtual screening of high-affinity
ATP competitive inhibitors against Human Lemur
Tyrosine Kinase-3 (LMTK3) domain- a novel
therapeutic target for breast cancer**

Structure based virtual screening of high-affinity ATP competitive inhibitors against Human Lemur Tyrosine Kinase-3 (LMTK3) domain- a novel therapeutic target for breast cancer

8.1. Abstract

In this work, we have studied the ATP binding mechanism with LMTK3 domain and also carried out virtual screening on LMTK3 domain to identify lead compounds using Dock blaster server. The top scored compounds obtained from Dock blaster were then narrowed down further to six lead compounds (ZINC37996511, ZINC83363046, ZINC3745998, ZINC50456700, ZINC83351792 and ZINC83364581) based on high binding affinity and non-bonding interactions with LMTK3 using Autodock4.2 program. We found in comparison to ATP, the lead compounds bind relatively stronger to LMTK3. The relative binding free energy results from MM-PBSA/GBSA method further indicate the strong binding affinity of lead compounds over ATP to LMTK3 in the dynamic system. Further, potential of mean force (PMF) study for ATP and lead compounds with LMTK3 have been performed to explore the unbinding processes and the free energy barrier. From the PMF results, we observed the lead compounds to have higher dissociation energy barriers than the ATP. Our findings suggest that these lead compounds may compete with ATP, and could act as probable potential inhibitors for LMTK3.

8.2. Introduction

We have already discussed about the LMTK3 and its implications in ER α positive breast cancer. And there are various endocrine therapies to treat ER α positive breast cancer [434,435]. The endocrine therapies have been found to be effective and also improve disease-free survival [286]. But then again, resistance commonly occurs against these therapies in ER α positive breast cancer due to the phosphorylation of ER α [31] by various protein kinases (MAPK, CDK2-CyclinA, and protein kinase A) [34-36] which module ER α transcriptional activity and alter its stability [288, 289]. Therefore,

protein kinases have been reported to be the key target in ER α positive breast cancer [290].

As that of other kinases, LMTK3 was also found to phosphorylate ER α and modulate its transcription activity and alter its stability [5-7] which leads to the breast cancer progression and endocrine therapy resistance, we have discussed this mechanism in Chapter 2 under section 2.3.4. Therefore, LMTK3 is considered to be an oncogenic protein and a new therapeutic target in breast cancer. Broad research on the identification of specific LMTK3 inhibitors is required to overcome breast cancer metastasis and endocrine resistance [109]. Though there are few studies on human LMTK3 binding characteristics [81, 436], we made an attempt to study the binding mechanism of LMTK3 domain in more detail to the extensive variation of binding specificity with different inhibitors.

We performed molecular docking of adenosine triphosphate (ATP) with LMTK3 domain to determine the ATP binding cavity in LMTK3. This information is critical to identify ATP competitive potential inhibitors against LMTK3 domain because most of the kinase inhibitors are known to compete for the ATP binding site [437,438]. Further, we made an attempt to screen lead compounds for LMTK3 from large library of ZINC database using Dock Blaster server [275]. Dock Blaster is a freely available online virtual screening server which has also been used to screen potential inhibitors in different protein targets [439-441]. Finally based on high binding affinity we arrived at top six lead compounds bound to the LMTK3 in the ATP binding pocket. Molecular dynamics simulations were carried out for LMTK3-ATP/lead compounds complexes in order to optimize the stability. Molecular Mechanics Poisson–Boltzmann or Generalized Born and surface area continuum solvation (MM-PBSA and MM-GBSA) [186, 187,188] method was used to calculate the binding free energy for LMTK3-ATP/lead complexes in order to refine and rescore the energy in dynamic system. We observed the lead compounds to bind strongly in the ATP binding pocket with high binding affinity than ATP. Furthermore, Potential of Mean Force (PMF) calculation was used to investigate the thermodynamics of dissociation of ATP and lead compounds from the binding pocket of LMTK3 domain. We found the lead compounds

to have higher dissociation energy barriers than the ATP. Our results as a whole suggest that the lead compounds considered in this work may be competent to ATP and could be useful in optimization and selection of therapeutic potential inhibitors for LMTK3.

8.3. Materials and Methods

8.3.1 Molecular docking and virtual screening

8.3.1.1. LMTK3-ATP docking

The protocol that we have used to dock ATP with LMTK3 has been discussed in Chapter 4 under section 4.3.5.

8.3.1.2. Virtual Screening and Molecular Docking of lead compounds for LMTK3 domain

Level I

Virtual screening was carried out with DOCK Blaster. DOCK Blaster is an online virtual screening server that picks and scores thousands of small molecules when user uploads a target protein structure. DOCK Blaster utilizes DOCK 3.6 for docking and ZINC database [276] for ligands. And it uses Pocket Picker (CLIPPERS) [277] to identify the binding pockets in the target protein. We submitted the modelled structure of LMTK3 domain to this server for virtual screening. From the large database, a small library of 200 compounds were screened based on molecular docking and energy score. The library contains the list of 200 hits with ZINC ID, DOCK score in kcal mol^{-1} , two-dimensional (2D) structure of the ligands that obeys the Lipinski rule [442].

Level II

The second level of screening was performed based on the best DOCK Blaster energy score and visual examination of ZINC lead compounds. We selected 100 hits based on binding energy score in the range between $-55 \text{ kcal mol}^{-1}$ to $-72 \text{ kcal mol}^{-1}$. Based on high DOCK Blaster score, PDB format for top 20 hits were downloaded for the third level for screening in Autodock4.2 program.

Level III

The third level of screening was performed based on the conformational docking for DOCK Blaster top 20 compounds in Autodock for the lead candidate identification. Input files of LMTK3 and lead compounds were prepared and saved in PDB format. The same docking procedure was used to dock these 20 lead candidates with LMTK3 that has been done to dock ATP. We obtained top 10 conformations for each hit; best docked conformation was evaluated based on least binding affinity value in kcal mol⁻¹ that possessed effective binding. All the docked conformations obtained from Autodock were visualized in LigPlot+ [254] to analyze hydrogen bonding interaction and hydrophobic interaction.

According to the Autodock score and physico-chemical properties (using Molinspiration web server <http://www.molinspiration.com>) of 20 lead compounds, we further narrowed down the hits from 20 to 6 top hits (ZINC37996511, ZINC83363046, ZINC3745998, ZINC50456700, ZINC83351792 and ZINC83364581) with least binding affinity values (-8.19, -8.08, -8.09, -5.73, 8.05, and -9.01) in kcal mol⁻¹. The summary of the overall computational virtual screening is shown in **Figure 9.1**. And the schematic representations of the chemical structure of the top six lead compounds are shown in **Figure 9.2**. LMTK3-ATP/lead compound complexes were taken as input for molecular dynamics simulations study.

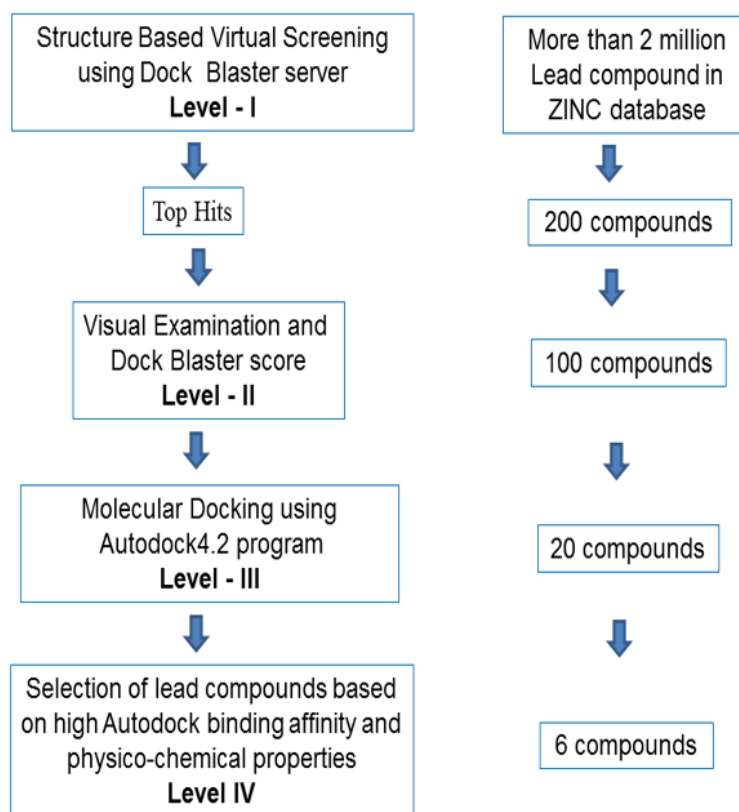


Figure 8.1. Flow chart of structure-based virtual screening of inhibitors obtained from ZINC database

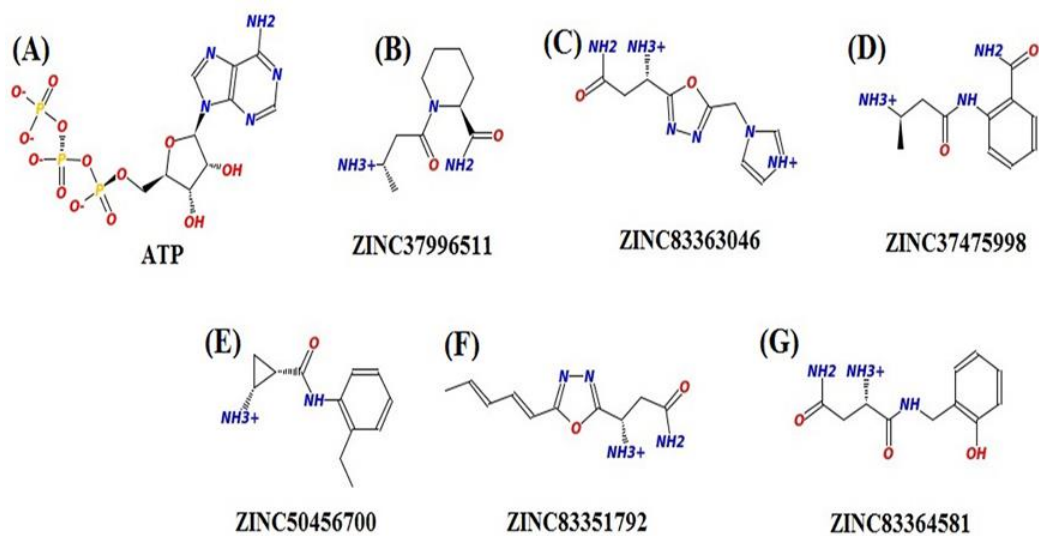


Figure 8.2. Chemical structures of ATP and lead compounds with zinc IDs

8.3.2. Molecular Dynamics (MD) simulation of LMTK3-ATP/lead complexes

We performed MD simulation for LMTK3-ATP/lead complexes, using the Particle Mesh Ewald Molecular Dynamics (PMEMD) [305] module of AMBER12 [122] software package. The partial charges and force field parameters for the ATP and lead compounds were generated automatically using the antechamber program [443] in AMBER12. Force field parameters were given for the ligand and the protein using the xleap module in AMBER12. General Amber force field (GAFF) [161] and AM1-BCC [444] charges were used for ligands, while AMBERff99SB force field was used for the protein. We obtained the initial coordinate and topology files for all the complex systems using xleap and antechamber module. The resultant initial structure of the individual system was solvated using TIP3P [167] water mode with the water box of size 10 \AA from the solute in the x, y, and z coordinates and then 3 sodium counter-ions were added to neutralize the protein. The potential energy of initial structures were minimized using 1000 steps of steepest descent followed by 2000 steps of conjugate gradient method. During the energy minimization, we fixed the protein molecule using harmonic constraints (excluding the water molecules) with a force constant of $30 \text{ kcal mol}^{-1} \text{ \AA}^2$ to overcome the bad contacts between water molecules and the protein. Second minimization was carried out without any constraints for 3000 cycles (1000 cycle of steepest descent and 2000 cycle of conjugate gradient). Then the complex systems were slowly heated from 0 to 300 K with a weak $20 \text{ kcal mol}^{-1} \text{ \AA}^{-2}$ constraints at 40 ps in NVT condition. This allows the systems to undergo slow relaxation. In MD simulation, using a geometrical tolerances of $5 \times 10^{-4} \text{ \AA}$, the SHAKE [165] constraints were imposed on all covalent bonds involving hydrogen atoms, with a time set to 2 fs. Then, equilibration and long production steps were performed in NPT condition ($T=300 \text{ K}$ and $P=1 \text{ atm}$) and temperature regulation was achieved with the help of Berendsen weak coupling method (0.5 ps time constant for heat bath coupling and 0.2 ps pressure relaxation time) [166]. Finally, for the analysis of conformational dynamics of LMTK3-ATP/lead complexes, we performed 15 ns long MD simulation at NPT condition using 1 ns heat bath coupling time constant. The analyses of structural convergence properties such as Root Mean Square Deviation (RMSD), Root Mean Square Fluctuation (RMSF) were carried

out using cpptraj [358] in AMBER12. For inspecting the 3D structure of the molecule, we used UCSF Chimera [180] and VMD [179].

8.3.3. Free Energy calculation of LMTK3-ATP/lead complex

8.3.3.1. MM-PBSA and MM-GBSA method

We have calculated the binding free energy of LMTK3-ATP/lead complexes using MM-PBSA/GBSA [186, 187, 188] method. From their corresponding MD simulation trajectories, we have extracted 200 snapshots and carried out MM-GBSA/PBSA calculations on the three components of all the complex system: (i) the protein LMTK3 (ii) ligand (ATP/lead compounds) and (iii) the complex (LMTK3-ATP/lead compounds). The interaction energy and solvation free energy were calculated for each of these components, and the averages of these results were considered to determine and evaluate the ligand-binding free energy. In general, the binding free energies in condensed phase can be calculated according to the equations that have been described in Chapter 3 under section 3.5.1.

8.3.3.2 Umbrella Sampling Simulations

We calculated the PMF for ATP and the lead compounds with LMTK3 using the Umbrella Sampling (US) simulations [183] with the weighted histogram analysis method (WHAM) [445, 185]. US simulations were performed in order to describe the unbinding pathway of each ligand from its binding site in LMTK3, which may be essential in revealing the inhibitor binding efficiency [446-448]. For the PMF analysis, distances between the ligand and LMTK3 were calculated as a function of all atoms of ligand and $C\alpha$ atoms of LMTK3. Umbrella samples were calculated by increasing and decreasing the center of mass distance between the ligand and LMTK3. Here based on MD simulation, several small windows were prepared along a predefined reaction path which depends on the exploration of phase space. We have incorporated biasing potentials (also known as harmonic potentials) [183] to restrict the molecular system to be in the specifically selected regions of phase space. This has been done for a number of windows. For each window, the biased probability distribution (histogram) for the equilibrated system is obtained. As a result, the most favorable free energy constant for

combined simulations is determined using WHAM. In US method, the restart file of the previous step was used as the input file for the configuration in both the increasing and decreasing cases. After an increment of 1 Å, windows were obtained. Here 1 ns NPT dynamics was performed for each window, where we used the resultant equilibrated structure as the starting coordinate for the next window. Later, NPT production run was performed to generate the data from collected trajectories. We applied harmonic potential with a spring constant of 2 kcal mol⁻¹Å².

8.4. Results and discussions

8.4.1. ATP binding pocket of LMTK3 domain

The ATP binding cavity in LMTK3 was determined by performing molecular docking in Autodock4.2. We obtained ten conformations of LMTK3-ATP docked complex. Among the ten conformations, the best conformation with a least binding energy (-1.71 kcal mol⁻¹) was chosen. The Autodock score and the amino acids of LMTK3 involved in interaction with the ATP have been depicted in **Table 8.1**. Using the Ligplot+ tool we have analysed the hydrogen bonding and hydrophobic interaction present in LMTK3-ATP complex as shown in **Figure 8.3A**. From the **Figure 8.3A**, we see residues Asp284 and Lys177 forming two hydrogen bonds with ATP while His264, His289, Ser290, Tyr185 forming one hydrogen bond with ATP and other residues involved in hydrophobic interaction.

We noticed that ATP is interacting with some of the residues present in the activation loop (that extends from 284 - 313) of LMTK3 (**Figure 8.4**). From the earlier studies [362, 71], we see that the activation loop of catalytically active kinase facilitates the protein substrates and ATP to bind. The activation loop (consisting of 20–35 amino acids) is more flexible and it is actually the sub-region of the activation segment. This activation loop region starts from the DFG motif and ends at APE, ALE or SPE motif [362, 71]. And it moves due to the rotation of the DFG motif from inactive (DFG-out, closed conformation) to active (DFG-in, open conformation) conformation [71]. But with respect to LMTK3, the activation loop starts from DYG instead of DFG and ends at APE motif [82, 361]. In our study we observed that as LMTK3 is DYG-in conformation, it opens the activation loop and forms a buried hydrophobic pocket where ATP binds (**Figure 8.4**) in a similar manner as that of other kinases [449, 450].

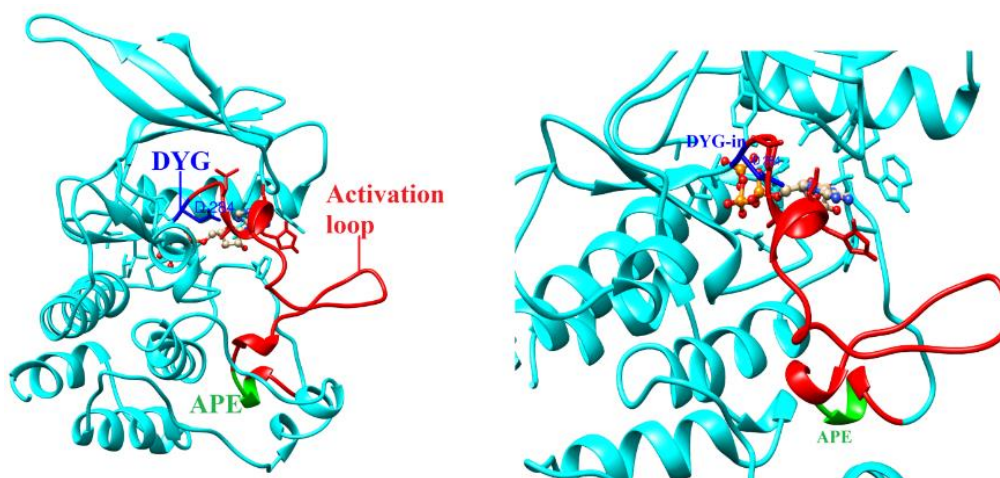


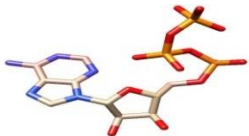
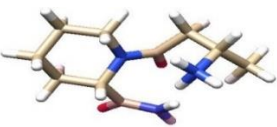
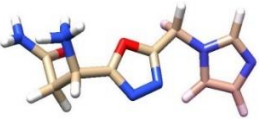
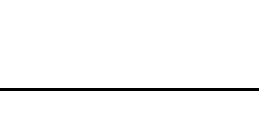
Figure 8.4. ATP binding pocket, where activation loop is in open conformation and form a pocket where ATP binds

8.4.2. Potential inhibitors for LMTK3

From the Dock Blaster, we arrived at 200 top hits for LMTK3 based on binding energy score (that comprises of electrostatic energy, VDW energy and desolvation energy) and Lipinski's rule of five. The top hit among the screened ZINC compounds were found to have a score of $-72.05 \text{ kcal mol}^{-1}$ and the last hit to have $-44.55 \text{ kcal mol}^{-1}$. All the ZINC compounds consist of rotatable bonds between 2 to 5 that showed the efficiency of ligands to be the key parameter involved in the docking. In the screening procedure, we

gradually narrowed down the hits from 200 to 100 then 100 to 20. From the 20 lead compounds, the top 6 hits were selected based on Autodock score and the physico-chemical properties obtained from Molinspiration server. The top six compounds (ZINC37996511, ZINC83363046, ZINC3745998, ZINC50456700, ZINC83351792 and ZINC83364581) show least binding energy value of -8.19, -8.08, -8.09, -5.73, -8.05, -9.01 kcal mol⁻¹ respectively. In addition, other energies like vdW+H-Bond+Desolvation energy and total internal energy in kcal mol⁻¹ also revealed the formation of LMTK3-lead compound complex with stronger affinity shown in **Table 8.2**. **Table 8.1** summarizes the autodock score of the ligands, interacting amino acids and number of hydrogen bond formed with the residues of LMTK3. Autodock results revealed that the compounds have high Autodock score than ATP.

Table 8.1. The Autodock score and amino acids of LMTK3 involved in hydrogen bonding interactions with ATP and other lead-compounds.

Protein	Ligands	Autodock score (kcal/mol)	Amino acids involved in hydrogen bonding	No. of hydrogen bonds
LMTK3	ATP 	-1.71	Ser290, Lys177, His264, Tyr262, His289, Asp284, Tyr185, Gly283	8
LMTK3	ZINC37996511 	-8.19	His264, Asp284, Asn271	5
LMTK3	ZINC83363046 	-8.08	Lys177, Tyr296, Glu181, Asp284, Asp266	6
LMTK3	ZINC37475998 	-8.09	Lys177, Asp284,	3

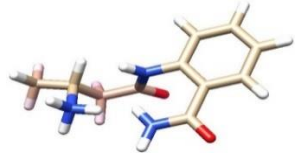

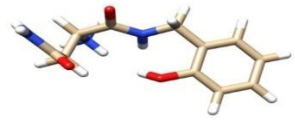
			Glu181	
LMTK3	ZINC505456700 	-5.73	Asp284, Asn271	2
LMTK3	ZINC83351792 	-8.05	Lys177, His264, Asp284, Asp266, Asn271, Tyr296	7

Table 8.2. AutoDock results of ATP and lead compounds

Parameters	ATP	ZINC 37996511	ZINC 83363046	ZINC 37475998	ZINC 50456700	ZINC 83351792	ZINC 83364581
Binding free Energy (kcal mol ⁻¹)	-1.71	-8.19	-8.08	-8.09	-5.73	-8.05	-9.01
VDW+Hbond+Desolv energy (kcal mol ⁻¹)	-5.58	-9.93	-10.29	-8.09	-6.75	-11.05	-10.52
Total internal Energy (kcal mol ⁻¹)	-1.12	-1.81	-1.46	-1.21	-1.41	-2.51	-3.54

Hydrogen and hydrophobic interaction between the LMTK3 and the lead compounds in the complex were determined using the Ligplot+ tool as shown in **Figure 8.3**. From the Ligplot+ analysis, we observed the lead compounds and ATP to have more or less similar interactions with LMTK3. All the six compounds exhibit hydrogen bonding

interaction with either of these residues: Asp284, Lys177, His264 which is also involved in hydrogen bonding with ATP. All the six lead compounds were observed to form hydrogen bonding with LMTK3 through Asp284 (**Figure 8.3 B-G**), compound (B) ZINC37996511 formed H-bond with His264, compound (F) ZINC83351792 and (G) ZINC83364581 formed H-bond with both Lys177 and His264, and compound (C) ZINC83363046, (D) ZINC37475998, formed H-bond with Lys177 (see **Fig. 8.3**). We infer that Asp284 residue in LMTK3 to be the key residue in the binding pocket. The binding modes of ATP and lead compounds with LMTK3 are shown in **Figure 8.5**. And the surface diagrams of docked structures are shown in **Figure 8.6**. From **Figure 8.4** and **Figure 8.6** we can say that the six lead compounds bind to the LMTK3 exactly at the same pocket where ATP binds and could be consider as potential ATP competitive inhibitors.

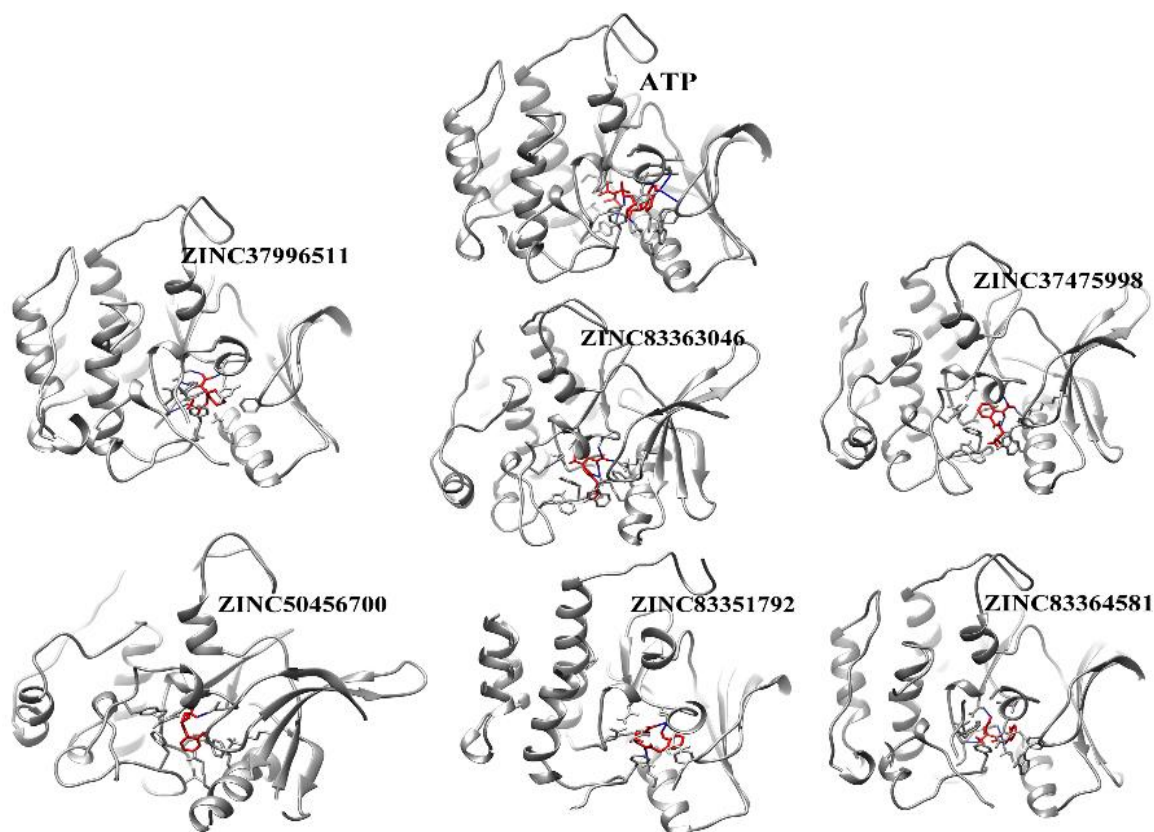


Figure 8.5. Binding modes of LMTK3 with ATP and lead compounds: ligands are shown in red color, hydrogen bonds between ligand and protein denoted in navy blue color.

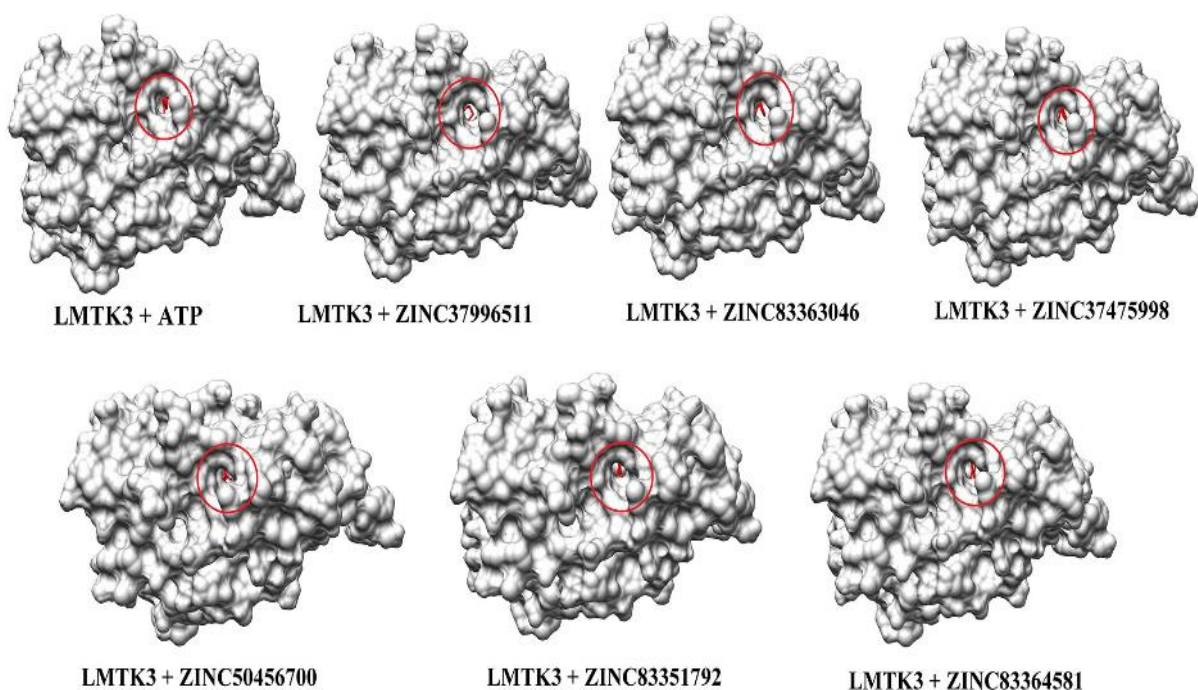


Figure 8.6. Surface diagram of binding cavity of complexes: *LMTK3-ATP* and *LMTK3-lead compounds*

Earlier reports have suggested that, most of the protein kinase inhibitors that have been currently accepted for clinical use, are found to bind on the catalytically active kinases at the ATP binding pocket, and those inhibitors are referred as type I inhibitors [451]. It is also seen that FDA-approved inhibitors to have a hydrophobic contact with residues that are positioned just before the DFG-D of the activation segment [451, 452]. Most of the inhibitors are known to interact with the DFG-D at the beginning of the activation segment and these contacts may vary and involve hydrophobic interactions, hydrogen bonds, salt bridges, and van der Waals contact distances [452]. In our study we also observed that all the six inhibitors are interacting (h-bonding or hydrophobic) with DYG-D (Asp-284) of the activation segment of LMTK3. We superimposed the entire inhibitor/ATP-LMTK3 complex together and observed that the inhibitors are binding in the ATP site and some of the activation loop residues are also interacting with the inhibitors as shown in **Figure 8.7**. We could therefore consider these inhibitors to be the Type I inhibitor. Development of specific kinase inhibitors always remain a

challenging task due to significant sequence similarity of amino acids among kinase family members mainly in the ATP binding pocket. Therefore, targeting the activation loop could be helpful in improving inhibitor selectivity and specificity because the activation loop region is less conserved in kinases [453].

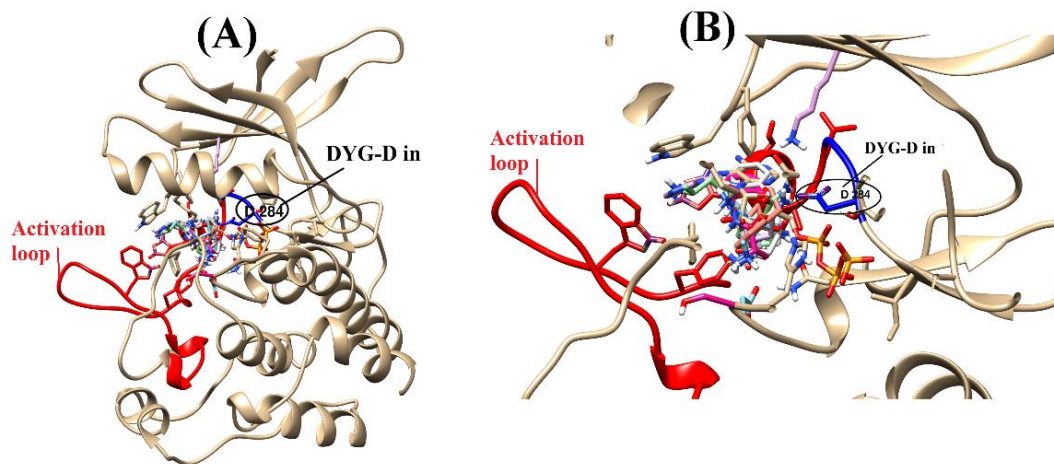


Figure 8.7. Superimposed LMTK3-ATP and inhibitor complex: (A) LMTK3 is DYG-D in conformation, open activation loop forming the binding pocket for ATP/inhibitors (B) Zoomed binding pocket, residues of activation loop protrude out and interacting with inhibitors

8.4.3. Bioavailability of LMTK3-inhibitors

The ADME properties are essential to evaluate these lead compounds for further applications. We used Molinspiration Cheminformatics web server (<http://www.molinspiration.com>) to calculate the ADME properties of these lead compounds based on the octanol-water partition coefficient and the topological polar surface area. The physico-chemical properties of the lead compounds are depicted in **Table 8.3**. Earlier reports suggest that the molecular polar surface area of a compound should be equal or less than 140 \AA^2 for oral bioavailability. We observed the calculated molecular polar surface area values for these ligands range between 57 to 128.73 \AA^2 , indicating oral bioavailability [454] of these compounds while the Octanol-water partition coefficient ($\log P^c$) values of these compounds follow the range that is not more than 3. It is additionally vital for the compounds to obey with the Lipinski's 'rule

of five' [455] for the consideration of further applications. Our compounds obey the rule of five, thus, can be investigated further.

Table 8.3 Physico-chemical properties of the lead compounds

Lead compounds	Molecular Weight	H – bond acceptor	H – bond donor	Log P ^c	Rotatable bonds	TPSA (Å ²)
ZINC 37996511	214.289	5	5	-2.84	3	91.05
ZINC 83363046	236.235	8	6	-4.62	5	128.73
ZINC 37475998	222.268	5	6	-2.81	4	99.83
ZINC50456700	204.273	3	4	-0.75	3	57
ZINC8331792	223.256	6	5	-3	5	109.66
ZINC83364581	238.267	6	7	-3.58	5	120.06

TPSA = Topological polar surface area; logP = octanol-water partition coefficients

8.4.4. MD simulation and free energy calculations

In order to investigate further applicability of the lead compounds as potential LMTK3 inhibitors, molecular MD simulations and the relative binding free energy calculations were performed. From MD simulations we checked the stability of LMTK3-ATP/lead compounds and illustrate the binding modes of the lead compounds with LMTK3 in dynamic system. The conformational dynamics of LMTK3-ligand complexes were analyzed from the Root Mean Square Deviation (RMSD) with respect to its reference structure was calculated. **Figure 8.8** demonstrates the RMSD of the protein for C α atoms as a function of time. The RMSD values are observed in between 2 Å to 3 Å for each complex and are quite stable after 3 ns, thus showing the stability in the structure of all the complex systems.

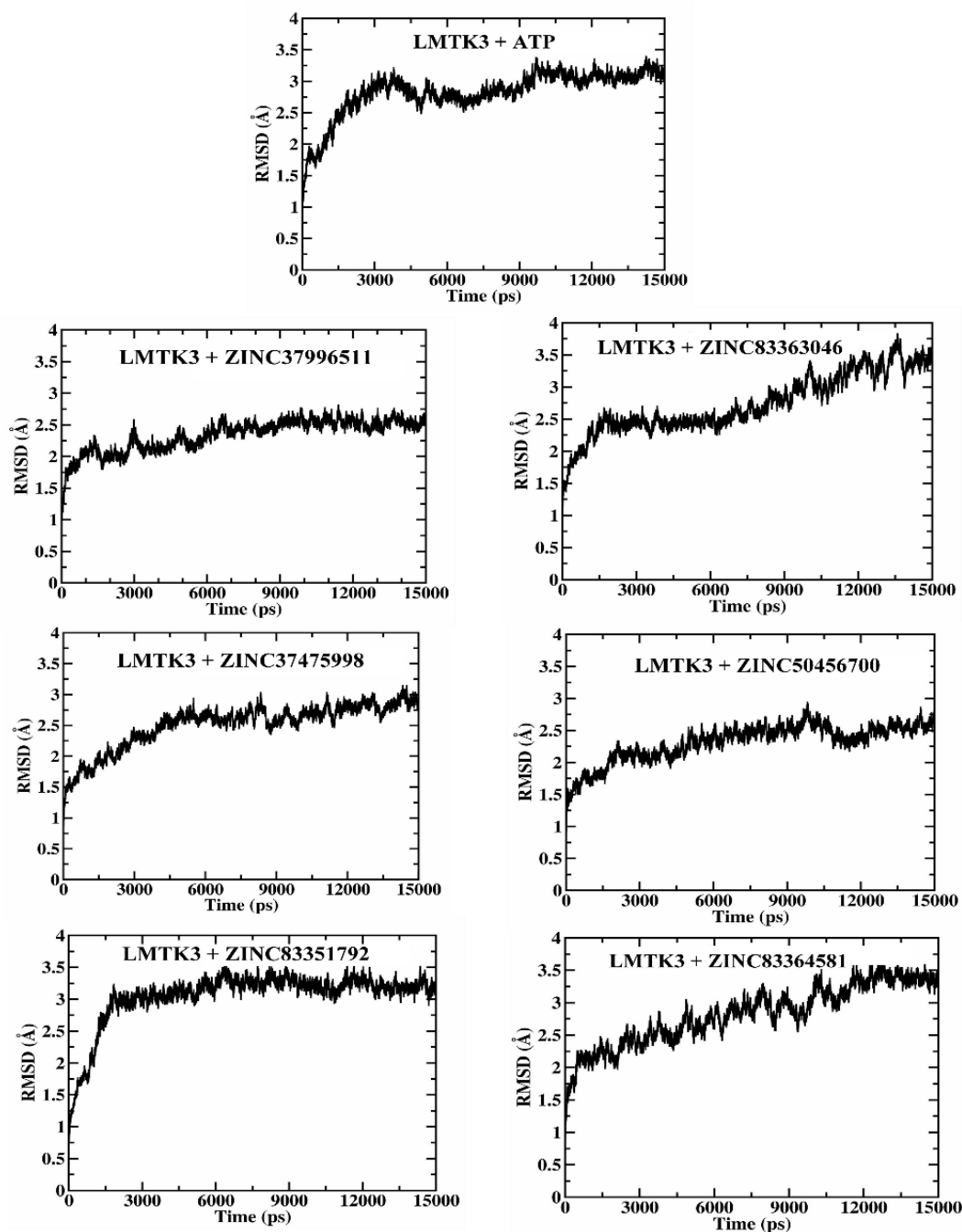


Figure 8.8. RMSD of ATP and six lead compounds to LMTK3 derived by molecular dynamics simulations

The flexibility of LMTK3-lead complexes was relatively lesser than the LMTK3-ATP complex. The Root Mean Square Fluctuation (RMSF) of every residue from its time – average position is shown in **Figure 8.9**. From the RMSF plots, fluctuations are observed to be in the loop regions of LMTK3-ATP/lead complexes. In addition we also

analyzed the intermolecular hydrogen bonds that illustrated the hydrogen-bonding pattern between LMTK3 and ATP/lead compounds in every frame of dynamic system (**Figure 8.10**). From the hydrogen bond analysis, we see that the lead compounds display appropriate number of hydrogen bonds in the dynamic system and correlated with the molecular docking results.

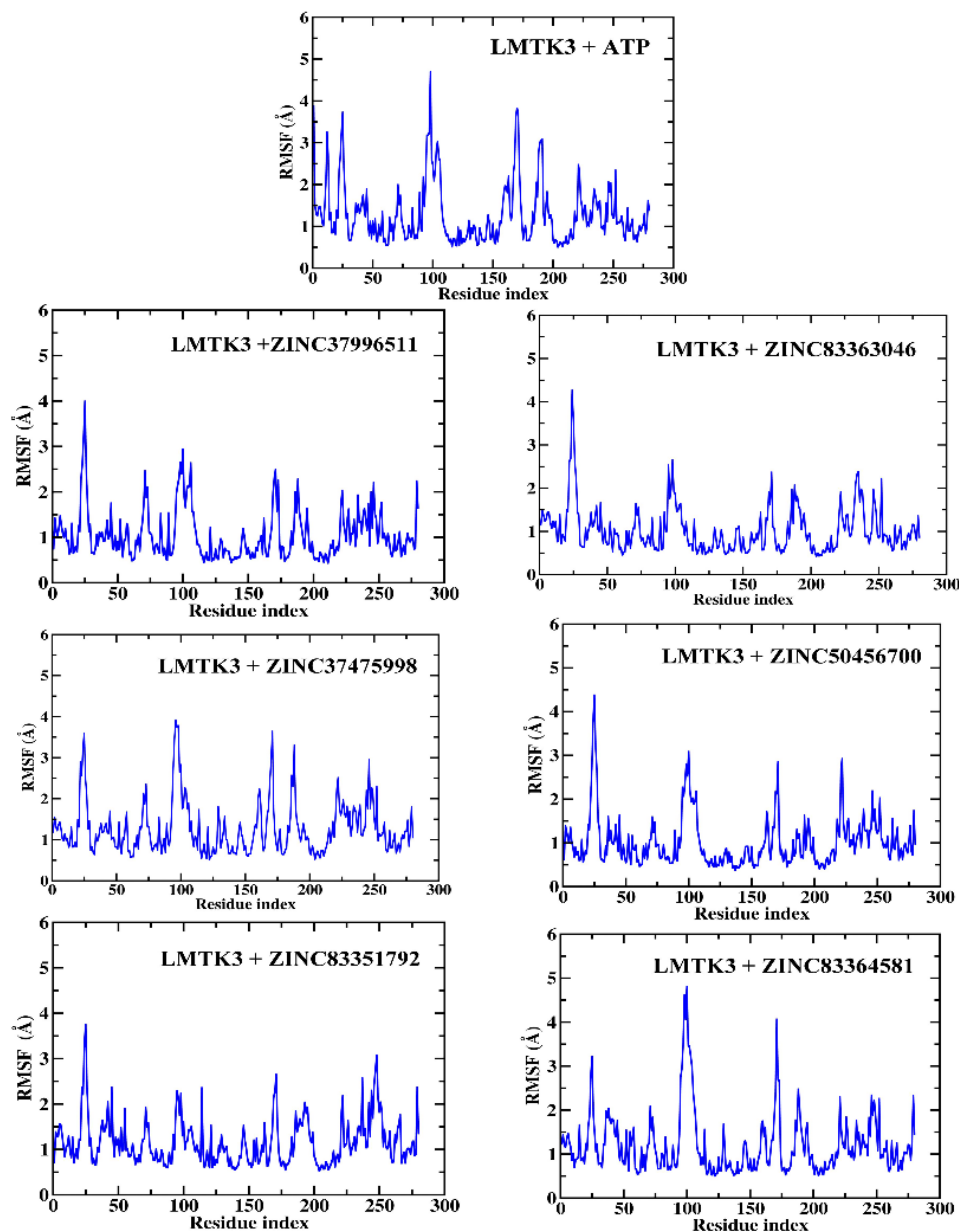


Figure 8.9. RMSF of ATP and six lead compounds to LMTK3 derived by molecular dynamics simulation

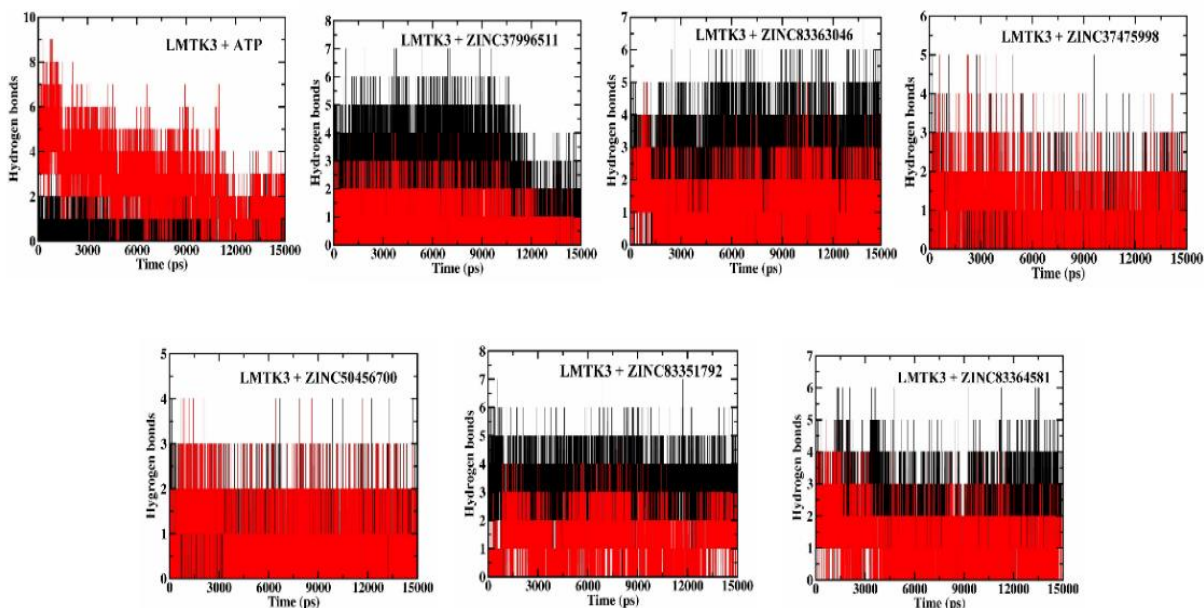


Figure 8.10. Number of intermolecular hydrogen bonds in LMTK3-ATP and LMTK3-lead compound complexes as a function of simulation time.

8.4.4.1. MM-PBSA/GBSA free energy calculation

The relative binding free energy and its corresponding components obtained from MM-PBSA/GBSA calculation for ATP and six lead compounds are listed in **Table 8.4**. From **Table 8.4**, the relative binding free energy of the ATP-LMTK3 complex using MM-PB/GBSA approach is found to be -7.61 (PBTOT) and -11.33 (GBTOT) kcal mol⁻¹. The $\Delta G_{\text{binding}}$ reveals that the formation of LMTK3-ATP/lead complexes is determined by the van der Waals (ΔE_{vdw}) interactions and the non-polar component of solvation energy (ΔG_{SA}).

Table 8.4. Binding free energy results of LMTK3-ATP/lead-compound complexes from MM-PBSA/GBSA calculations

	ATP	ZINC-37996511	ZINC-83363046	ZINC-37475998	ZINC-50456700	ZINC-83351792	ZINC-83364581
ELE	-356.86	-61.46	-45.11	-35.33	-37.17	-80.15	-62.06
VDW	-51.95	-36.77	-36.71	-30.21	-36.64	-24.97	-37.19
INT	-0.00	-0.00	0.00	-0.00	-0.00	-0.00	0.00
GAS	-408.80	-98.23	-81.82	-65.54	73.82	-105.12	-99.25

PB _{SUR}	-4.31	-2.39	-2.95	-3.09	-2.86	-3.08	-2.57
PB _{CAL}	405.50	69.52	54.83	46.84	53.09	95.64	67.54
PB _{SOL}	401.19	67.13	51.88	43.75	50.23	92.56	64.96
PB _{ELE}	48.65	8.06	9.72	11.51	15.92	15.49	5.48
PB_{TOT}	-7.61	-31.10	-29.95	-21.79	-23.58	-12.56	-34.28
GB _{SUR}	-4.31	-2.39	-2.95	-3.09	-2.86	-3.08	-2.57
GB	401.78	63.91	47.90	40.75	41.55	80.19	-62.49
GB _{SOL}	397.47	61.52	44.95	37.66	38.70	77.11	59.91
GB _{ELE}	44.93	2.45	2.79	5.42	4.38	0.04	0.43
GB_{TOT}	-11.33	-36.71	-36.88	-27.88	-35.12	-28.01	-39.34

ELE = electrostatic energy as calculated by the MM force field; **VDW** = van der Waals contribution from MM; **INT** = internal energy arising from bond, angle, and dihedral terms in the MM force field. (this term always amounts to zero in the single trajectory approach); **GAS** = total gas phase energy (sum of **ELE**, **VDW**, and **INT**); **PB_{SUR}/GB_{SUR}** = non-polar contribution to the solvation free energy calculated by an empirical model; **PB_{CAL}/GB_{CAL}** = the electrostatic contribution to the solvation free energy calculated by PB or GB; respectively. **PB_{SOL}/GB_{SOL}** = sum of non-polar and polar contributions to solvation; **PB_{ELE}/GB_{ELE}** = sum of the electrostatic solvation free energy and MM electrostatic energy; **PB_{TOT}/GB_{TOT}** = final estimated binding free energy calculated from the terms above. (kcal mol⁻¹)

In case of LMTK3-lead complexes, $\Delta G_{\text{binding}}$ varies from -12.56 to -34.28 kcal mol⁻¹ using the MM-PBSA method where as in MM-GBSA method $\Delta G_{\text{binding}}$ varies from -28.01 to -39.34 kcal mol⁻¹. The high negative total binding free energy is favourable in the formation of LMTK3-lead complexes in dynamic system and also infers the stability of the complexes. We noticed all the lead compounds have the higher total binding free energy thus have stronger binding affinity with LMTK3 than ATP. Therefore we expect these lead compounds may be competitive to ATP and could be used to inhibit LMTK3.

8.4.4.2. Umbrella Sampling

Umbrella sampling (US) simulations were performed to illustrate the unbinding pathway of each one of these lead compounds and ATP from the LMTK3 domain. For this study, the equilibrated complex structures of LMTK3-ATP/lead compounds were chosen as the initial conformation for the US simulations. The convergence of the PMFs

for each system was assured by performing 1 ns US simulations for each window. As shown in **Figure 8.11**, the PMF depths from the US simulations of LMTK3-lead complex systems were observed to be much higher than LMTK3-ATP complex, which shows a deeper energy potential depth and thus a longer residence time of ligands in the binding pocket of LMTK3.

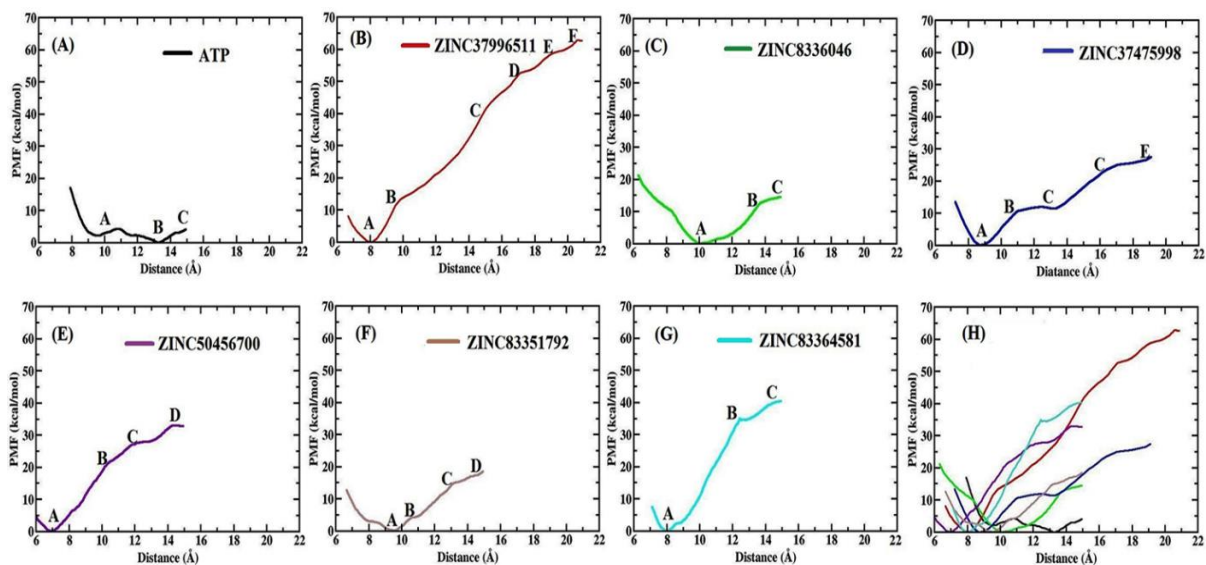


Figure 8.11. Unbinding process of ATP/lead compounds dissociating from the ATP binding site of LMTK3 domain

The comparative study of PMF curves designated that different reaction coordinates (RCs) were employed when ligands dissociate from the ATP binding pocket of LMTK3. For instance, different phases of vertical elevation of the PMF (**Figure 8.11**) are observed for different ligands (lead compounds) when moves out of the ATP binding pocket of LMTK3. With the increase of the biased potential, ligands move out of the ATP binding pocket. For example in case of the compound (ZINC37996511, **Figure 8.11 B**), upgrading of the PMF (region A–B, B–C, C–D, D–E, E–F) of RCs are observed when ligand moves out of binding pocket of LMTK3 and finally at 20 Å of RC, the ligand totally dissociate with a high potential energy value of 62 kcal mol⁻¹. Similarly, the other lead compounds also show, with the elevation of the PMF curve, the ligands eventually moves out of the binding pocket (**Figure 8.11**). In case of the unbinding of ATP from the binding pocket of LMTK3, we noticed an energy barrier first appear at point C of the PMF profile (11 Å of the RC in **Figure 8.11 A**) and finally

at 14.3 Å of RC, ATP totally dissociate from its binding site very easily than the other lead compounds with a less potential energy value of 5 kcal mol⁻¹.

We have compared the PMF profiles of all the lead compounds and ATP with LMTK3. PMF plots (**Figure 8.11 A-G**) depicted that among all the ligands studied here, ATP has the lowest dissociation energy barrier, therefore estimated to get released from the ATP binding site of LMTK3 with ease. By comparing all the PMF plots, we obtained the order of lowest dissociation energy barrier of our potential inhibitors (lead compounds) from ATP binding site of LMTK3 to be ATP < ZINC83363046 < ZINC83351792 < ZINC37475998 < ZINC50456700 < ZINC83364581 < ZINC37996511.

8.5. Conclusions

Using virtual screening and molecular docking we have narrowed down six lead compounds for LMTK3 and found that the lead compounds were bound to LMTK3 at the same binding pocket (involving residues Asp284, Lys177, His264) where ATP binds. From the molecular dynamics simulation study, MM-GBSA/PBSA, and PMF analysis, we observed LMTK3-ATP/lead compounds to be stable in the dynamics system, and the lead compounds ZINC37996511, ZINC83363046, ZINC37475998, ZINC50456700, ZINC83351792, and ZINC83364581 were bound to LMTK3 with high affinity than ATP. And also from calculated PMF values, we noticed the lead compounds to have higher dissociation energy barriers than ATP. Though these compounds do not share structure and shape similarity with ATP but they are found to compete with the ATP binding site and act as potential drug candidates for LMTK3. Further, an energy optimized pharmacophore modelling approach may be required to identify and design effective LMTK3 inhibitors.